Voltage Clamp Fluorimetry Reveals a Novel Outer Pore Instability in a Mammalian Voltage-gated Potassium Channel

Moninder Vaid,[1] Thomas W. Claydon,[1] Saman Rezazadeh,[1] and David Fedida[1,2]

[1]Department of Anesthesiology, Pharmacology, and Therapeutics, and [2]Department of Cellular and Physiological Sciences, University of British Columbia, Vancouver, B.C. V6T 1Z3, Canada

Voltage-gated potassium (Kv) channel gating involves complex structural rearrangements that regulate the ability of channels to conduct K^+ ions. Fluorescence-based approaches provide a powerful technique to directly report structural dynamics underlying these gating processes in *Shaker* Kv channels. Here, we apply voltage clamp fluorimetry, for the first time, to study voltage sensor motions in mammalian Kv1.5 channels. Despite the homology between Kv1.5 and the *Shaker* channel, attaching TMRM or PyMPO fluorescent probes to substituted cysteine residues in the S3–S4 linker of Kv1.5 (M394C-V401C) revealed unique and unusual fluorescence signals. Whereas the fluorescence during voltage sensor movement in *Shaker* channels was monoexponential and occurred with a similar time course to ionic current activation, the fluorescence report of Kv1.5 voltage sensor motions was transient with a prominent rapidly dequenching component that, with TMRM at A397C (equivalent to *Shaker* A359C), represented 36 ± 3% of the total signal and occurred with a τ of 3.4 ± 0.6 ms at +60 mV ($n = 4$). Using a number of approaches, including 4-AP drug block and the ILT triple mutation, which dissociate channel opening from voltage sensor movement, we demonstrate that the unique dequenching component of fluorescence is associated with channel opening. By regulating the outer pore structure using raised (99 mM) external K^+ to stabilize the conducting configuration of the selectivity filter, or the mutations W472F (equivalent to *Shaker* W434F) and H463G to stabilize the nonconducting (P-type inactivated) configuration of the selectivity filter, we show that the dequenching of fluorescence reflects rapid structural events at the selectivity filter gate rather than the intracellular pore gate.

INTRODUCTION

Voltage-gated potassium (Kv) channels control excitability by gating the passage of repolarizing K^+ current across the cell membrane. Kv channel gating involves complex voltage- and time-dependent structural events that regulate the ability of channels to conduct K^+ ions. In response to depolarization, alterations in the structure of the voltage-sensing domains initiate conformational changes at the intracellular pore gate that lead to channel opening and ion flux. In some channels these events trigger time-dependent rearrangements at the outer mouth of the pore that collapse the ion conduction pathway and lead to channel inactivation. Detailed dynamic structural information is required to understand the mechanisms of these gating processes in different Kv channels.

Fluorescence-based methods have allowed direct observation of ion channel gating conformations. Using voltage clamp fluorimetry (VCF) and the archetypal *Shaker* Kv channel, simultaneous recording of ionic current along with changes in fluorescence emission from tetramethylrhodamine-5-maleimide (TMRM) attached in the S3–S4 linker has shown that the fluorescence changes provide a faithful report of the time and voltage dependence of voltage sensor movements (Mannuzzu et al., 1996; Cha and Bezanilla, 1997; Pathak et al., 2007). Two sites in particular in the S3–S4 linker, M356 and A359, have proven particularly useful in fluorimetric studies. Similar fluorescence reports of voltage sensor dynamics have also been described in hSkM1 Na^+ channels, hERG, eag and BK_{Ca} K^+ channels, and HCN channels (Cha et al., 1999; Smith and Yellen, 2002; Bannister et al., 2005; Savalli et al., 2006; Bruening-Wright et al., 2007).

In addition to the observation of voltage sensor motions, some of these fluorescence studies report additional conformational changes that occur after channel activation. These rearrangements reflect transitions that are associated with opening of the channel and/or collapse of the outer pore during inactivation. TMRM attached within the S3–S4 linker of the *Shaker* channel detects not only the independent movement of the voltage sensors, but also conformational rearrangements

M. Vaid and T.W. Claydon contributed equally to this manuscript.
Correspondence to David Fedida: fedida@interchange.ubc.ca

Abbreviations used in this paper: 4-AP, 4-aminopyridine; PyMPO, 1-(2-maleimidylethyl)-4-(5-(4-methoxyphenyl)oxazol-2-yl)pyridinium methanesulfonate; TMRM, tetramethylrhodamine-5-maleimide; VCF, voltage clamp fluorimetry.

T.W. Claydon's present address is School of Kinesiology, Simon Fraser University, Burnaby, V5A 1S6 Canada.

The Rockefeller University Press $30.00
J. Gen. Physiol. Vol. 132 No. 2 209–222
www.jgp.org/cgi/doi/10.1085/jgp.200809978

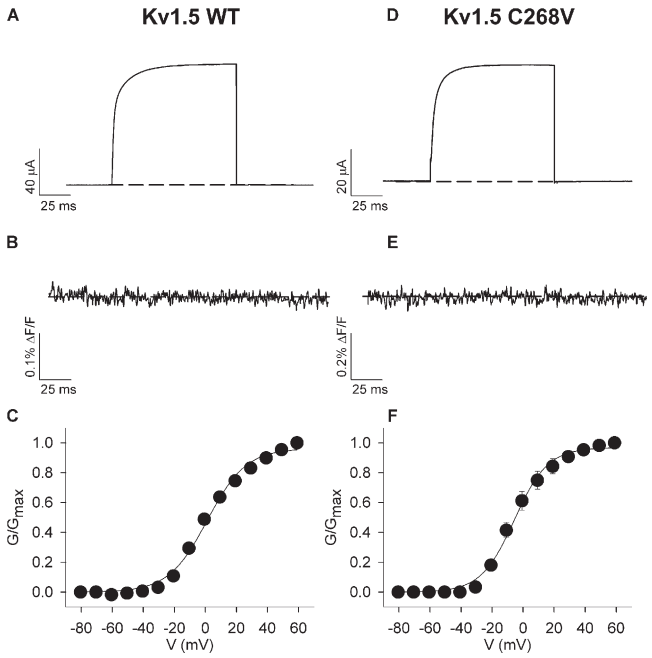

Figure 1. TMRM fluorescence from Kv1.5 WT and Kv1.5 C268V channels. (A, B, D, and E) Ionic current (A and D) and fluorescence (B and E) traces recorded from oocytes expressing Kv1.5 WT (A and B) or Kv1.5 C268V (D and E) channels labeled with TMRM. Voltage clamp pulses were applied from −80 to +60 mV in 10-mV increments (100 ms duration) from a holding potential of −80 mV (only +60 mV traces are shown for clarity). (C and F) Mean G-V relations for Kv1.5 WT (C; $n = 9$) and Kv1.5 C268V (F; $n = 4$). $V_{1/2}$ and k values for the G-V relation of Kv1.5 channels were 1.2 ± 1.3 and 12.5 ± 1.0 mV, respectively. The $V_{1/2}$ and k values for the G-V relations of Kv1.5 C268V were −5.7 ± 1.0 and 10.8 ± 0.8 mV, respectively. The $V_{1/2}$ values for the G-V relations of Kv1.5 WT and Kv1.5 C268V are significantly different $P < 0.01$ (unpaired t test). Note that error bars generally fall within the plotted points in C and F.

that are coupled with the concerted opening of the intracellular pore gate (Pathak et al., 2005). A number of sites within the S3–S4 linker also report the slow collapse of the outer pore that occurs during P/C-type inactivation (Loots and Isacoff, 1998, 2000; Gandhi et al., 2000; Claydon et al., 2007a,b). In addition, while some sites in the S3–S4 linker of BK_{Ca} channels report on the rapid voltage sensor movement during activation, other sites report slower rearrangements that may reflect transitions between multiple open states (Savalli et al., 2006). In hERG channels, slow TMRM fluorescence emission from E518, E519, and L520 reflects the slow activation of the voltage sensors in these channels. In some cases there is a fast fluorescence report, which is also observed in gating current measurements (Piper et al., 2003), with similar kinetics to channel inactivation, which may therefore report structural changes that are coupled in some way to the inactivation process (Smith and Yellen, 2002).

In the present study, we provide the first fluorescence reports of the dynamic gating events in mammalian Kv1 channels. The crystal structures from Kv1.2 (Long et al., 2005a) and the recent paddle-chimaera channel Kv2.1/Kv1.2 (Long et al., 2007), which are the closest structures that we have to Kv1.5, suggests that like *Shaker*, only sites L396 and A397 of Kv1.5 would be in the S4 α helix. However, previous work suggests that the entire S3–S4 region in Kv2.1 analogous to Kv1.5 from M394C to A397C would fall into the S4 α helix (Li-Smerin et al., 2000). Nevertheless, like in *Shaker*, robust fluorescence signals could be recorded from these two sites, M394C and A397C. Unexpectedly though, despite the high sequence homology between *Shaker* and Kv1.5 channels, the fluorescence report of voltage sensor motions upon activation from TMRM attached in the S3–S4 linker of Kv1.5 channels revealed unique and complex fluorescence changes. The fluorophore in Kv1.5 reports a novel rapid dequenching of fluorescence that occurs upon depolarization. Using 4-aminopyridine (4-AP) and the ILT triple mutation (V407I/I410L/S414T) to uncouple voltage sensor activation from opening of the intracellular pore gate, we demonstrate that this rapid unquenching of the fluorescence signal is associated with channel opening. Furthermore, by raising the external K^+ concentration, or introducing the W472F and H463G mutations, or the outer pore mutation, R487V, which all regulate or immobilize the outer pore gate while sparing normal functioning of the intracellular pore gate, we show that the unique fluorescence component measured in Kv1.5 channels is associated with gating at the selectivity filter.

MATERIALS AND METHODS

Molecular Biology

The vector pEXO was used to express Kv1.5 and *Shaker* Δ6-46 channels in *Xenopus laevis* oocytes. Cysteine residues were introduced at specific sites (M394C to V401C in Kv1.5, A359C in *Shaker*) in the S3–S4 linker for TMRM labeling and the only externally accessible cysteine residue, found in the S1–S2 linker, was replaced with a valine residue (C268V in Kv1.5, C245V in *Shaker*) to prevent nonspecific dye labeling. The deletion mutation Δ6-46 was introduced into *Shaker* channels to remove fast inactivation (Hoshi et al., 1990). The W472F mutation (equivalent to W434F in *Shaker* channels) was introduced to permanently inactivate channels (Perozo et al., 1993; Yang et al., 1997). To dissociate voltage sensor movement from channel opening, the ILT triple mutation (V407I, I410L, and S414T) was introduced in the S4 domain (Smith-Maxwell et al., 1998a,b). The R487V outer pore mutation (equivalent to T449V in *Shaker*) was introduced to inhibit inactivation (Lopez-Barneo et al., 1993), and the H463G mutation was introduced to accelerate P/C-type inactivation (Jäger and Grissmer, 2001). Point mutations were generated using the Stratagene Quikchange kit (Stratagene) using primers synthesized by SigmaGenosys, and were sequenced at the University of British Columbia core facility. cRNA was synthesized using the mMessage mMachine T7 Ultra transcription kit (Ambion) from linearized (*Sac II*) cDNA template.

Oocyte Preparation

Xenopus laevis oocytes were prepared and isolated as described previously (Claydon et al., 2007a). Following removal of the follicular

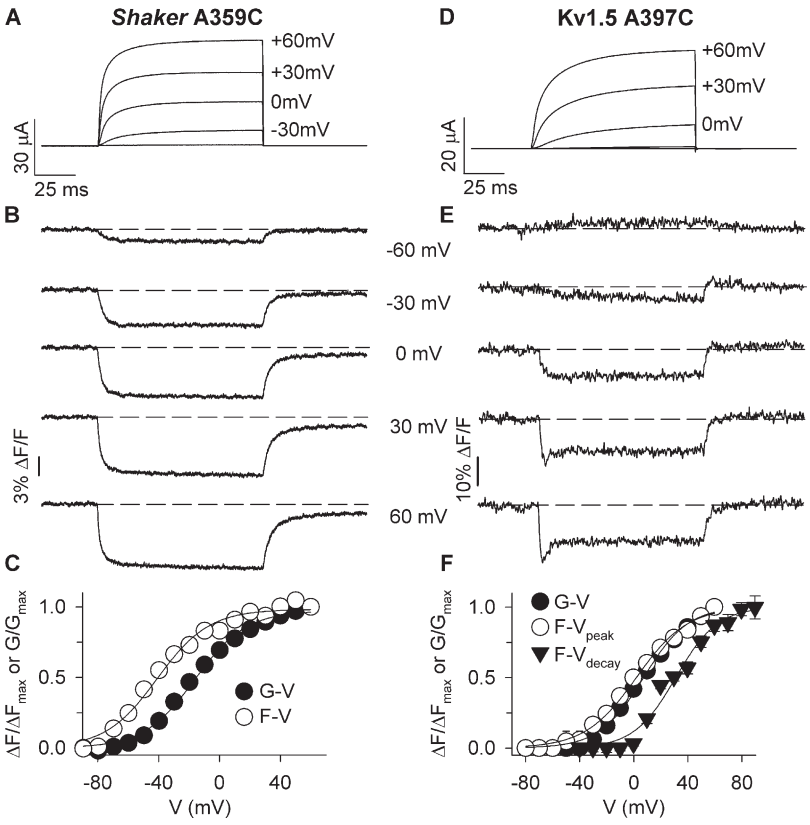

Figure 2. Characteristics of the TMRM fluorescence report from Kv1.5 A397C channels. (A, B, D, and E) Representative ionic current (A and D) and fluorescence (B and E) traces recorded from oocytes expressing *Shaker* A359C (A and B) or Kv1.5 A397C (D and E) channels labeled with TMRM. Voltage clamp pulses were applied from −80 to +60 mV in 10-mV increments (100 ms duration) from a holding potential of −80 mV (only highlighted traces are shown for clarity). (C and F) Mean G-V and F-V relations for *Shaker* A359C (C; $n = 3$) and Kv1.5 A397C (F; $n = 4$). $V_{1/2}$ and k values for the G-V relation of *Shaker* A359C channels were −16.2 ± 1.3 and 16.8 ± 1.1 mV, respectively, and the corresponding values for the F-V relation were −40.9 ± 1.9 and 17.0 ± 1.7 mV, respectively. $V_{1/2}$ and k values for the G-V relation of Kv1.5 A397C were 7.3 ± 1.6 and 16.4 ± 1.2 mV, respectively, and the corresponding values for the F-V_{peak} relation were 1.9 ± 1.9 and 19.0 ± 1.3 mV, respectively. The F-V_{peak} relation was not significantly shifted from the G-V relation. The voltage dependence of the dequenching component of fluorescence from Kv1.5 A397C (calculated as the peak minus end fluorescence amplitude, F-V_{decay}) is also shown in F; $V_{1/2}$ and k values were 31.0 ± 2.4 and 15.5 ± 1.9 mV, respectively.

layer, oocytes were injected with 50 nl (10–200 ng) of cRNA and incubated in Barth's solution, which contained (in mM) 88 NaCl, 1 KCl, 2.4 $NaHCO_3$, 0.82 $MgSO_4$, 0.33 $Ca(NO_3)_2$, 0.41 $CaCl_2$, 20 HEPES (pH 7.5), for 1–5 d at 19°C. Injected oocytes were labeled with 5 µM TMRM or 1-(2-maleimidylethyl)-4-(5-(4-methoxyphenyl) oxazol-2-yl) pyridinium methanesulfonate (PyMPO) in depolarizing solution, which contained (in mM) 99 KCl, 1 $MgCl_2$, 2 $CaCl_2$, and 5 HEPES (pH 7.5), for 30 min at 10°C. Unless stated, all chemicals were purchased from Sigma-Aldrich.

Two Electrode Voltage Clamp Fluorimetry

Ionic currents and fluorescence signals were recorded simultaneously using two electrode voltage clamp fluorimetry as described previously (Claydon et al., 2007a). The bath solution contained (in mM) 96 NaCl, 3 KCl, 1 $MgCl_2$, 0.3 $CaCl_2$, and 5 HEPES (pH 7.5). Voltage-dependent fluorescence changes were measured from TMRM or PyMPO fluorophores attached at specific sites in the S3–S4 linker. In the case of TMRM, excitation and emission light were filtered with 525-nm bandpass and 560-nm longpass filters, respectively. For PyMPO, 425-nm bandpass filter and 515-nm longpass emission filters were used. Emitted light was detected using a 9124b Electron Tubes photomultiplier tube. Acquired signals (ionic current and fluorescence) were sampled at 20 kHz and filtered off-line at 1–3 kHz unless otherwise stated. Fluorescence traces recorded from TMRM represent the average of five sweeps (the interpulse interval was 2 s) unless stated otherwise. Fluorescence traces recorded from PyMPO represent the average of three sweeps because of rapid bleaching of the fluorophore. Microelectrodes containing 3 M KCl with a resistance of 0.2–0.8 MΩ were used. Working concentrations of 4-AP were diluted from a 100 mM stock solution made with ND96 solution and titrated to pH 7.5.

Data Analysis

Conductance–voltage (G-V) and fluorescence–voltage (F-V) relations were fitted with a single Boltzmann function: $y = 1/1 (1 + \exp(V_{1/2} - V)/k)$, where y is the conductance or fluorescence amplitude normalized with respect to maximal conductance or fluorescence amplitude, $V_{1/2}$ is the half-activation potential, V is the test voltage, and k is the slope factor. Channel conductance was derived using the normalized chord conductance from isochronal current measurement (internal K^+ was assumed to be 98 mM). Data are shown as mean ± SEM. Statistical differences were assessed using Student's t test.

RESULTS

The Fluorescence Report of Voltage Sensor Movement in Kv1.5 Channels Is Unique

Kv1 channels have an extracellular cysteine residue in the S1–S2 linker that is a potential site for TMRM labeling and that may fluoresce in addition to any site that is engineered in the S3–S4 linker for gating studies. Control experiments in Fig. 1 showed that neither wild-type Kv1.5 (Fig. 1, A–C), nor Kv1.5 C268V (Fig. 1, D–F), showed a fluorescence report upon depolarization despite large expressed current amplitudes (Fig. 1, A and D). The G-V relations are shown in Fig. 1 (C and F) and the $V_{1/2}$ and k values were 1.2 ± 1.3 and 12.5 ± 1.0 mV for wild type and −5.6 ± 1.0 and 10.8 ± 0.8 mV for C268V. All subsequent fluorescence experiments were performed using the Kv1.5 C268V mutation in addition to a fluorophore site as stated.

Dynamic changes in the fluorescence report from TMRM attached within the S3–S4 linker at A359C in *Shaker* channels provide a faithful report of the time and

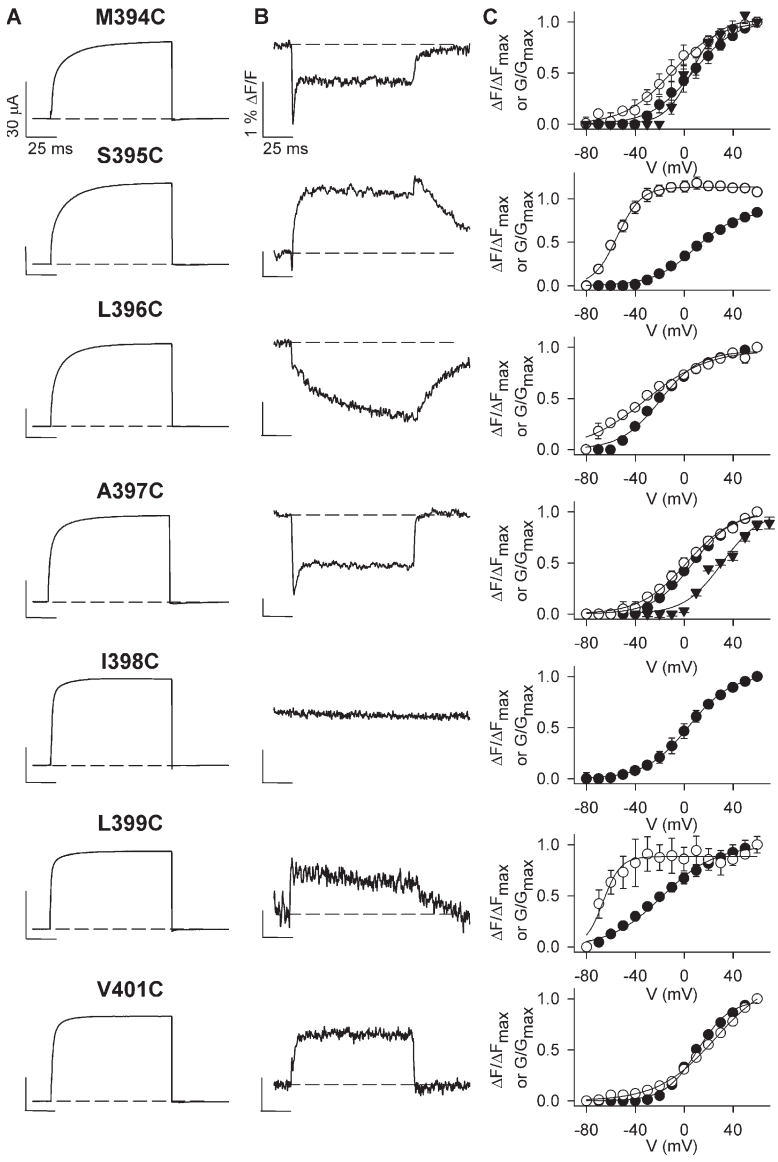

Figure 3. Sites facing the pore report the rapid dequenching of fluorescence. (A and B) Representative ionic and fluorescence signals recorded from TMRM attached at each site in the Kv1.5 S3–S4 linker from M394C to V401C during 100 ms voltage clamp pulses from −80 to +60 mV. Scale bars represent 30 μA currents (A) and 1% ΔF/F fluorescence deflections (B), respectively. (C) Mean G-V (●) and F-V (○) relations for each mutation. Boltzmann fits of the data gave $V_{1/2}$ and k values for G-V and F-V relations of 6.9 ± 1.9 and 17.3 ± 1.4 mV (G-V), respectively, and −10.5 ± 1.9 and 19.4 ± 1.4 mV (F-V), respectively, for M394C (n = 4); 9.0 ± 1.4 and 17.2 ± 1.0 mV (G-V), respectively, and −54.7 ± 0.8 and 9.7 ± 0.7 mV (F-V), respectively, for S395C (n = 7); −19.7 ± 1.8 and 16.2 ± 1.5 mV (G-V), respectively, and −31.5 ± 3.3 and 25.1 ± 2.8 mV (F-V), respectively, for L396C (n = 3); 7.4 ± 1.6 and 16.4 ± 1.2 mV (G-V), respectively, and 2.0 ± 1.9 and 18.9 ± 1.3 mV (F-V), respectively, for A397C (n = 4); −18.1 ± 3.4 and 21.6 ± 2.7 mV (G-V), respectively, and −66.4 ± 1.6 and 7.2 ± 1.5 mV (F-V), respectively, for L399C (n = 3); 10.8 ± 1.2 and 13.3 ± 0.9 mV (G-V), respectively, and 25.7 ± 2.2 and 23.3 ± 1.0 mV (F-V), respectively, for V401C (n = 7); voltage-dependent fluorescence deflections were not evident with TMRM attached at I398C, and R400C channels did not express ionic current. The voltage dependence of the dequenching component of fluorescence (calculated as the peak minus end fluorescence amplitude) is also shown (▼) for M394C and A397C. In the case of M394C, $V_{1/2}$ and k values were 5.8 ± 1.8 and 10.9 ± 1.5 mV (n = 4), respectively, and the corresponding values for A397C were 31.0 ± 2.4 and 15.5 ± 1.9 mV (n = 4).

voltage dependence of voltage sensor motions induced by changes in the transmembrane potential (Mannuzzu et al., 1996; Cha and Bezanilla, 1997; Pathak et al., 2007). Fig. 2 (A–C) shows a characteristic example of the fluorescence reports from *Shaker* A359C during 100-ms voltage clamp pulses to a range of potentials. Simultaneous recordings of ionic current (Fig. 2 A) and TMRM fluorescence (Fig. 2 B) show that the fluorophore in *Shaker* reports a monoexponential quenching upon depolarization that occurs with a time course (τ = 2.4 ± 0.5 ms at +60 mV) that is similar to, but faster than, that of the activation of ionic current (τ = 4.5 ± 1.0 ms at +60 mV; n = 4). The conformational changes reported by the fluorophore display a voltage dependence ($V_{1/2}$ = −40.9 ± 1.9 mV) that is ∼25 mV left shifted from the G-V relation ($V_{1/2}$ = −16.2 ± 1.3 mV; Fig. 2 C), as is expected for movement of the voltage sensors in advance of channel opening. Similar monoexponential reports of voltage sensor movement that precede at least one component of ionic current activation kinetics have also been reported in hERG, eag, BK_{Ca}, and HCN channels (Smith and Yellen, 2002; Bannister et al., 2005; Savalli et al., 2006; Bruening-Wright et al., 2007). Many of the clearest recordings in the above studies have come from *Shaker* A359C or M356C, or the equivalent residues to those in other channels (e.g., L520C in hERG channels; Smith and Yellen, 2002).

In Fig. 2 (D–F), we show, for the first time, the fluorescence report of voltage sensor movement in a mammalian Kv1 channel, Kv1.5. The fluorescence report is from TMRM attached at A397C, which is the equivalent S3–S4 linker site to A359C in *Shaker* channels. In contrast to the monoexponential time course of the fluorescence quenching from *Shaker* (Fig. 2 B) and other Kv channels (Smith and Yellen, 2002; Bannister et al., 2005; Savalli et al., 2006), TMRM attached at Kv1.5 A397C

reported a unique profile of fluorescence change (Fig. 2 E). Upon depolarization, the fluorescence quenching deflection from Kv1.5 A397C was rapid, but transient with a prominent dequenching component that reached a steady-state level by the end of the 100-ms voltage pulse. The recovering component of fluorescence was only observable at relatively depolarized potentials and became faster and larger with stronger depolarizations. Another difference from *Shaker* A359C (Fig. 2 C) was that the F-V relation of Kv1.5 A397C fluorescence, taken from the peak of the fluorescence deflections, was not significantly left shifted ($V_{1/2}$ = 1.9 ± 1.9 mV) from the G-V relation ($V_{1/2}$ = 7.3 ± 1.6 mV; Fig. 2 F). Furthermore, the voltage dependence of the dequenching component amplitude was actually right-shifted ($V_{1/2}$ = 31.0 ± 2.4 mV) from the G-V relation (Fig. 2 F). These observations suggest that at least some component of the fluorescence deflection from TMRM attached at Kv1.5 A397C may be coupled in some way with channel opening.

Spectroscopic Mapping of Kv1.5 Voltage Sensor Dynamics—Discrete vs. Global Rearrangements

The different report of fluorophore environmental change observed in Kv1.5 (Fig. 2, D–F) may suggest that very different voltage sensor conformational changes occur in these channels than in *Shaker* channels. However, a fluorescence scan of the S3–S4 linker of Kv1.5 (Fig. 3) reveals that the complex structural changes are only reported by TMRM at two sites, A397C and M394C. This cannot be accounted for by differences in ionic current waveforms (Fig. 3 A) or changes in the G-V relationships with the different linker mutants (Fig. 3 C), since these all appear similar. Both A397C and M394C report a voltage-dependent acceleration of the dequenching component and an increase in its contribution to the total fluorescence change upon depolarization (Fig. 4). Other sites in the scan do not report the rapid component of fluorescence and produce deflections that are, in general, similar to those described from the equivalent sites in *Shaker* channels (Gandhi et al., 2000; Pathak et al., 2007). This suggests that Kv1.5 voltage sensor movement per se is not dissimilar to that of *Shaker* channels. Furthermore, given that the functional data suggests that the C-terminal end of the S3–S4 linker likely adopts an α-helical structure, placing M394C and A397C on the same side of the helix, (Li-Smerin et al., 2000; Gonzalez et al., 2001; Li-Smerin and Swartz, 2001), and at least M394C and A397C sense the same microenvironment changes, these data suggest that the fluorescence changes represent local protein rearrangements rather than global reconfigurations. Since M394C and A397C come close to the pore domain upon depolarization (Gandhi et al., 2000; Elinder et al., 2001), we hypothesized that TMRM attached at M394C or A397C might be reporting on an additional structural rearrangement that is associated with opening of the pore.

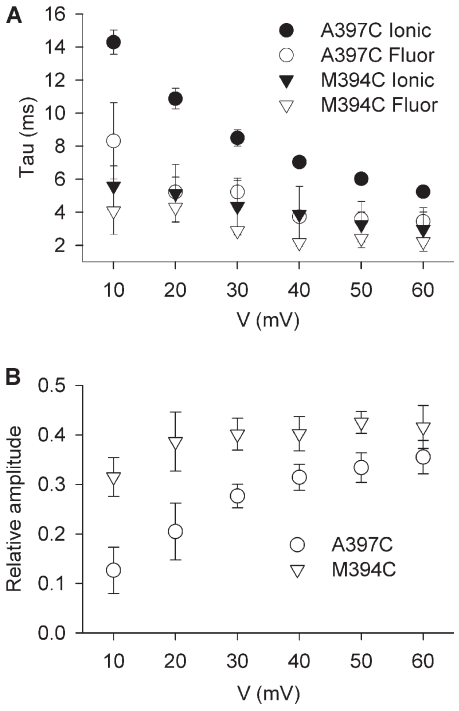

Figure 4. Voltage dependence of the dequenching of fluorescence and ionic current activation. (A) Mean values for the time constants of the dequenching component of fluorescence measured from TMRM attached to either M394C or A397C and the time constants of the associated ionic current activation, measured between +10 and +60 mV. (B) Relative amplitude of the dequenching component of fluorescence, normalized to the total fluorescence deflection on depolarization, measured from TMRM attached at either M394C or A397C.

In support of this, the time constant data in Fig. 4 A show a reasonably good match between the time constants of channel activation (filled symbols) and the fast component of fluorescence dequenching, especially for M394C (open triangles).

A similar fluorescence profile of channel gating was reported by another fluorophore, PyMPO (Fig. 5), that has different physical and spectral properties to TMRM. Ionic currents (Fig. 5 A) and the G-V relationship (Fig. 5 C), which had a $V_{1/2}$ and k of 2.3 ± 1.9 and 17.8 ± 1.3 mV, respectively, were relatively unaffected by labeling with PyMPO. The fluorescence reports were very similar to those seen with TMRM, and included a transient component that appeared at around 0 mV, a potential at which significant numbers of channels opened (Fig. 5 B). It was noted that PyMPO fluorescence recordings bleached more rapidly during clamp pulses, and perfect baseline correction was not possible when full F-V relations were obtained. This explains the baseline drift seen in recordings at 0 and +30 mV in Fig. 5 B. With TMRM, the time constant of the fluorescence dequenching at +60 mV was 3.4 ± 0.6 ms and it represented 36 ± 3% of the total signal (Fig. 4; n = 4). The corresponding values with PyMPO were similar (Fig. 5 D); the time

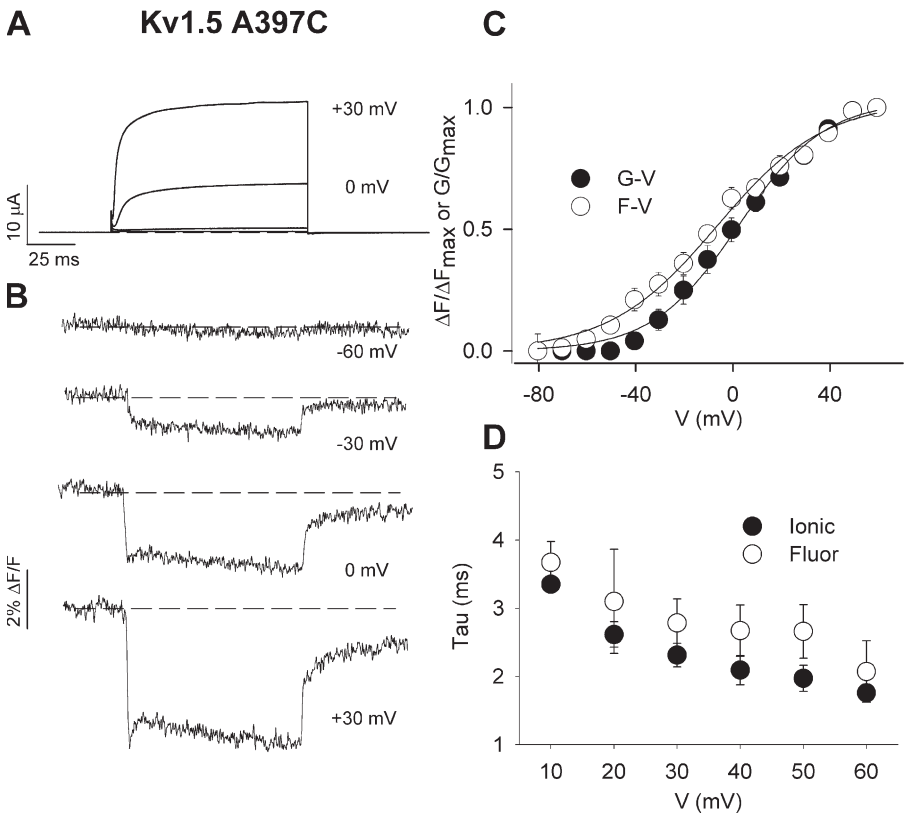

Figure 5. Other fluorophores report the unusual fluorescence signal. (A and B) Ionic current (A) and fluorescence (B) traces recorded from oocytes expressing Kv1.5 A397C channels labeled with PyMPO. Voltage clamp pulses were applied from −80 to +60 mV in 10-mV increments (100 ms duration) from a holding potential of −80 mV (only traces at −60, −30, 0, and +30 mV are shown). (C) Mean G-V and F-V relations for Kv1.5 A397C labeled with PyMPO ($n = 4$). Boltzmann fits of the data gave $V_{1/2}$ and k values for G-V and F-V relations of 2.3 ± 1.9 and 17.8 ± 1.3 mV (G-V), respectively, and −6.5 ± 2.5 and 22.2 ± 1.7 mV (F-V), respectively. (D) Mean values for the time constants of the dequenching component of fluorescence measured from PyMPO attached to A397C and the time constants of the associated ionic current activation. The time constants show similar voltage dependence at test voltages ranging from +10 to +60 mV.

constant was 2.1 ± 0.5 ms and it represented 25 ± 8% of the total signal ($n = 3$), suggesting that the fluorescence changes observed are a faithful report of protein conformational changes. Upon repolarization, the return of both the TMRM and PyMPO fluorescence signals was rapid (see also Fig. 2 E), and showed no evidence of return of the rapid component of fluorescence. This suggests that the motions represented by the dequenching of fluorescence upon depolarization are slow to recover upon repolarization.

The Dequenching Component of Fluorescence Is Associated with Transitions to the Open State

As a first test of this hypothesis, we compared the effect of the holding potential on the fluorescence report from Kv1.5 A397C channels (Fig. 6). If the transient dequenching component of fluorescence is associated with late transitions to the open state rather than voltage sensor transitions early in the activation pathway, the fluorescence report from channels that open from hyperpolarized potentials (i.e., −120 mV) should be the same as that from channels opening from preactivated states (i.e., −40 mV). Data in Fig. 6 A shows ionic currents and fluorescence signals from TMRM attached at A397C recorded during a test pulse applied immediately after a conditioning pulse to either −120 or −40 mV. The ionic current records show that channel opening was more rapid following a conditioning pulse to −40 mV, which collects channels in preactivated states, than following a pulse to −120 mV, which collects channels in early closed states. Consistent with this, the fluorescence signal recorded following a prepulse to −40 mV dequenched more rapidly than following a pulse to −120 mV. However, the unique fluorescence profile that we observed in Kv1.5 channels was maintained following a prepulse to −40 mV, and the relative amplitude of the rapid fluorescence dequenching was unchanged by alterations in the holding potential (Fig. 6 B).

As a further test of this hypothesis, we investigated the effects of preventing opening on the fluorescence report from Kv1.5 A397C channel. We measured the fluorescence report in the presence of 10 mM 4-AP or the ILT triple mutation (V407I, I410L, S414T), both of which dissociate voltage sensor movement from channel opening by stabilizing channels in preopen closed states (McCormack et al., 1994; Smith-Maxwell et al., 1998a,b; del Camino et al., 2005; Pathak et al., 2005). 10 mM 4-AP reduced the ionic current by about two thirds and abolished the rapid component of fluorescence (Fig. 7, A and B), reverting the fluorescence phenotype to that reported by *Shaker* A359C (compare the fluorescence trace in the presence of 4-AP with that in Fig. 2 B). In addition, 4-AP restored the left-shifted voltage dependence of the F-V relation (the $V_{1/2}$ of the F-V was ∼41 mV left shifted from that of the G-V; Fig. 7 C). In a similar manner, at potentials (e.g., +60 mV) that stabilize ILT mutant channels in the activated-not-open state (del Camino et al., 2005), where little ionic current is

observed (Fig. 7 D), the dequenching component of fluorescence from Kv1.5 ILT A397C channels was abolished and the *Shaker*-like monoexponential report of voltage sensor movement was rescued (Fig. 7 E). The F-V relation in ILT mutant channels was also left shifted from the G-V relation (the $V_{1/2}$ of the F-V was -41.6 ± 1.8 mV; Fig. 7 F). These data clearly demonstrate that the dequenching component of fluorescence from A397C is associated with channel opening. Furthermore, these results show that the depolarized position of the F-V relation in Fig. 2 F does not reflect the true voltage dependence of voltage sensor movement, because it is influenced by an event that TMRM detects upon channel opening.

The Dequenching Component of Fluorescence Does Not Reflect Gating at the Intracellular Pore Gate

The observation in Fig. 2 E that the fluorescence signal does not report the return of the dequenching component upon repolarization suggests that the protein motions reported upon are relatively slow to recover. To investigate the time course of the recovery, we performed a double pulse protocol in which we applied a 75-ms test pulse to +60 mV at increasing intervals following a 15-ms conditioning pulse to +60 mV (Fig. 8 A). The dequenching phase of fluorescence was relatively slow to recover as shown in Fig. 8 B. After 7.5 ms repolarization, the amplitude of dequenching in the test pulse was significantly reduced, but increased with increasing rest interval duration. The time dependence of the return of the rapid component is plotted in Fig. 8 C, and the time constant for the return was 20.7 ± 3.7 ms ($n = 3$). This is significantly slower than the time constant of intracellular pore gate closure during deactivation in Kv1.5 channels, which is ~5 ms at these potentials (Chen et al., 1997), but since the experiments in Fig. 8 were performed in 3 mM extracellular K^+, it was not possible to resolve the time course of the decay of the tail currents directly at −80 mV. However, the time course of recovery of the instantaneous ionic current level from the same experiments is a reasonable index of channel closing, indicated by the dotted line in Fig. 8 A. The mean data show a recovery time constant of 10.7 ± 0.8 ms ($n = 3$), which is significantly faster than the recovery of fluorescence ($P < 0.05$).

The slow return of the fluorescence upon repolarization suggests that although associated with channel opening, the dequenching component of fluorescence does not reflect gating of the intracellular pore. We also observed that the recovery of this phase was dependent upon the conditioning pulse duration (Fig. 9). Following longer conditioning pulses (15 ms; Fig. 9 A) that allowed significant channel opening, the dequenching component was almost absent in the first test pulse, whereas following shorter conditioning pulses (5 ms; Fig. 9 B) that restricted channel opening, there was a robust component in the first test pulse. These data further demonstrate that the slowly recovering fluorescence dequenching is related to channel opening. Based on these data, we considered that the rapid fluorescence changes might reflect structural events occurring at the outer pore gate upon opening.

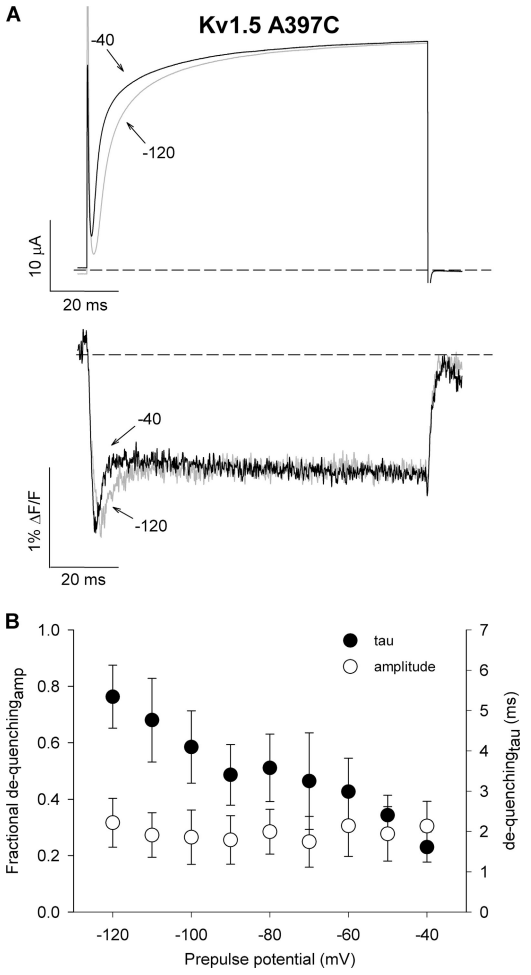

Figure 6. The dequenching of fluorescence is associated with late transitions in the activation pathway. (A) Ionic currents and fluorescence signals recorded from TMRM attached at A397C during a 100-ms test pulse to +60 mV following a 100-ms conditioning pulse to either −120 or −40 mV. The dequenching component of fluorescence remains robust in channels that activate from preactivated states, suggesting that the dequenching component does not reflect voltage sensor transitions early in the activation pathway. (B) Mean values for the time constant and relative amplitude of the dequenching component of fluorescence during a test pulse to +60 mV from a range of prepulse potentials ($n = 3$).

The Dequenching Component of Fluorescence Is Associated with Structural Events at the Selectivity Filter Gate

Although our experiments with 4-AP suggest that prevention of channel opening prevents the structural events reported by the fluorophore at A397C, drug binding

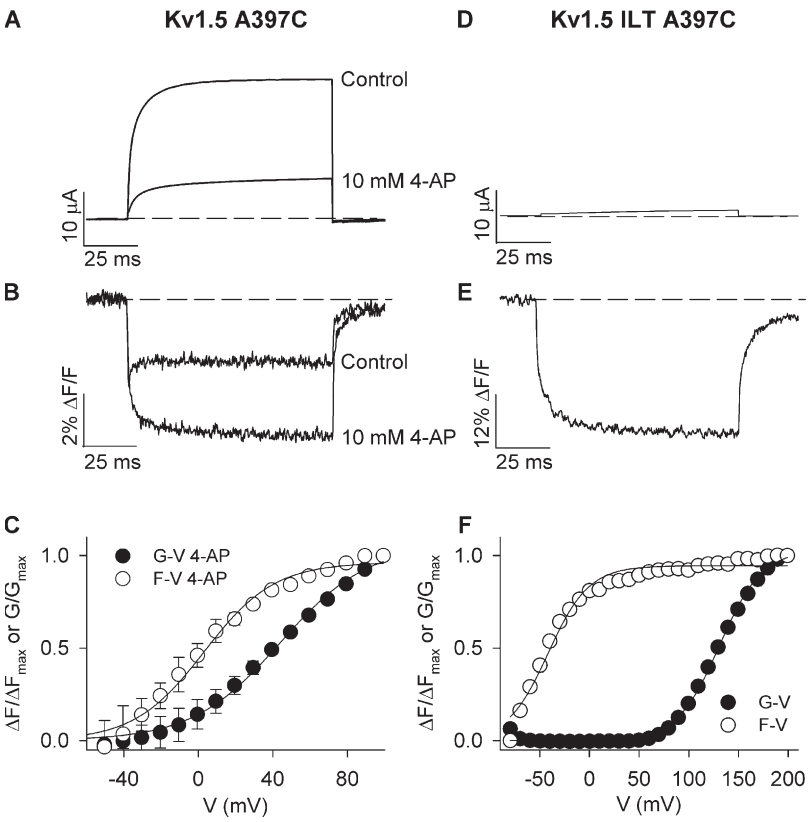

Figure 7. Prevention of opening abolishes the dequenching of fluorescence. (A and B) Ionic (A) and fluorescence (B) signals recorded from TMRM attached at A397C in control conditions and in the presence of 10 mM 4-AP during 100-ms voltage clamp pulses from −80 to +60 mV. 10 mM 4-AP prevented channel opening and reduced current amplitude by 66 ± 6% (n = 3). (C) Mean G-V and F-V relations in the presence of 10 mM 4-AP. $V_{1/2}$ and k values for G-V and F-V relations were 44.0 ± 2.8 and 23.6 ± 1.7 mV (G-V), and 3.2 ± 2.5 and 18.8 ± 2.1 mV (F-V; n = 3). The F-V relation was 41 mV left shifted from the G-V relation. (D and E) Representative ionic (D) and fluorescence (E) signals recorded from A397C in the presence of the ILT mutation during 100-ms voltage clamp pulses to +60 mV. The ILT mutation uncouples independent voltage sensor movement from the concerted opening transition (Smith-Maxwell et al., 1998a,b) resulting in a shift of the G-V relation to depolarized potentials (see F). (F) Mean G-V and F-V relations for Kv1.5 A397C ILT channels. $V_{1/2}$ and k values for G-V and F-V relations were 131.0 ± 1.2 and 21.4 ± 0.8 mV (G-V), respectively, and −41.6 ± 1.8 and 20.6 ± 1.7 mV (F-V; n = 3). The F-V relation was therefore 173 mV left shifted from the G-V relation.

also prevents selectivity filter gating events, including inactivation (Castle et al., 1994; Claydon et al., 2007a). In the ILT experiments it was difficult to assess whether the function of the selectivity filter inactivation gate of ILT channels is still intact at the strongly depolarized potentials (>+150 mV) required to drive channels into the open state, as activation was still slow at the maximum potentials studied in the experiments. Therefore, further experiments were performed using interventions and mutations known to affect the inactivation process or modulate outer pore gating in Kv1 channels, while measuring the fluorescence report from A397C.

There is strong evidence for a K^+ modulatory site within the outer pore of Kv channels that, when occupied, prevents collapse of the selectivity filter, acting with a "foot-in-the-door" mechanism (Pardo et al., 1992; Lopez-Barneo et al., 1993; Baukrowitz and Yellen, 1995; Rasmusson et al., 1995; Kiss and Korn, 1998). In some Kv1 channels, including Kv1.5 (Fedida et al., 1999), this regulation does not appear to be as strong as in *Shaker* channels, but raising the extracellular K^+ did significantly modulate the fluorescence report (Fig. 10). The ionic current amplitudes and time course are relatively unchanged at +60 mV, despite the reduction in driving force, as reported before for some Kv1 channels (Pardo et al., 1992). The fluorescence signals in Fig. 10 B show that raising the external K^+ concentration to 99 mM abolished the dequenching component and restored more of a *Shaker*-like fluorescence report of voltage sensor movement. The fluorescence report is not identical to that in *Shaker* (Fig. 2), though, and appears to show both a fast and slow component of quenching, but with 99 mM K^+ the left-shifted F-V relation of voltage sensor movement ($V_{1/2}$ = −36.4 ± 1.2 mV) becomes apparent (Fig. 10 C; n = 3). Clearly, K^+ regulation at an outer pore site is able to modulate the fluorescence environment change detected at A359C, and allow detection of voltage sensor movement.

To test outer pore regulation in another way, we introduced the mutation W472F, which is the equivalent to W434F in the *Shaker* channel, and which immobilizes the selectivity filter gate in a permanently nonconducting state in both *Shaker* (Perozo et al., 1993; Yang et al., 1997) and Kv1.5 channels (Wang et al., 1999; Wang and Fedida, 2001). Importantly, this mutation is not thought to immobilize the intracellular activation gate, as shown previously (Starkus et al., 1998). The tracings in Fig. 10 D show that although no ionic current was seen with this mutant, large fluorescence deflections were observed. In addition, the transient fluorescence change and thus structural events reported by the fluorescence at A397C were abolished. Taken together, these data strongly suggest that the dequenching component of fluorescence reported by TMRM attached at Kv1.5 A397C reflects rapid structural events at the selectivity filter gate that occur upon opening.

Closure of the selectivity filter gate underlies P/C-type inactivation in Kv channels (De Biasi et al., 1993;

Lopez-Barneo et al., 1993; Yellen, 1998; Kiss et al., 1999; Kurata and Fedida, 2006; Cordero-Morales et al., 2007). Although the time course of the fluorescence dequenching in Fig. 2 E is very rapid (3.4 ms at +60 mV) compared with the time course of P/C-type inactivation, which occurs in the order of seconds, we considered whether the novel fluorescence report from TMRM attached at A397C might reflect selectivity filter rearrangements that are associated in some way with inactivation. To test this, we examined the effects on the rapid component of fluorescence in Kv1.5 channels of the introduction of the outer pore mutation R487V (equivalent to T449V in *Shaker*), which is known to inhibit P/C-type inactivation in *Shaker* (Lopez-Barneo et al., 1993), and to abolish inactivation in Na^+-conducting Kv1.5 channels (Wang et al., 2000a,b). Data in Fig. 11 (A and B) show a typical ionic current and fluorescence signal recorded from TMRM attached at A397C in Kv1.5 R487V mutant channels during a 100-ms voltage clamp pulse to +60 mV. The tracing clearly shows that the dequenching component of fluorescence is maintained in the R487V mutation.

Other mutations in *Shaker* channels that modulate slow inactivation include E418 and V463 (Hoshi et al., 1991; Larsson and Elinder, 2000), but unfortunately we were unable to obtain current expression or fluorescence recordings in oocytes from the equivalent residues E456Q or E456C in Kv1.5 (see also Eduljee et al., 2007), or the equivalent residues to V463 in *Shaker*. However, another residue that modulates P/C-type inactivation in Kv1.5 is the His in the pore turret (Kehl et al., 2002). This mutation accelerated P/C-type inactivation as seen in the current record in Fig. 11 C, and also resulted in very low current expression levels, which was almost certainly due to both accelerated open-state and closed-state inactivation of the large population of the channels that do not pass current, as reported from our group and others previously (Jäger and Grissmer, 2001; Kehl et al., 2002; Zhang et al., 2005). This conclusion is supported by the robust fluorescence report from these channels (Fig. 11 D). This mutation completely removed the rapid dequenching phase of fluorescence at all potentials and showed a slow second phase of fluorescence quenching that matches the accelerated current inactivation seen in Fig. 11 C. The result suggests that collapse or immobilization of the selectivity filter gate before channel opening in H463G, as also seen in W472F (Fig. 10 D), prevents the structural change that causes the rapid fluorescence dequenching and allows unimpeded detection of voltage sensor movement.

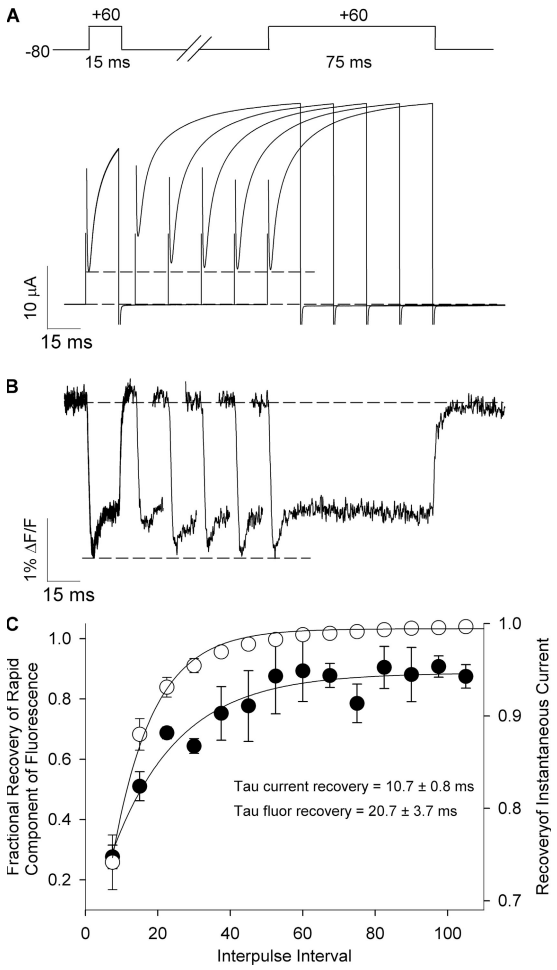

Figure 8. Time course for the recovery of the de-quenching component of fluorescence. (A and B) Ionic current and fluorescence signals recorded during the voltage protocol shown. The time course of the recovery of the dequenching component fluorescence amplitude was assessed during 75-ms test pulses to +60 mV applied at different intervals following a 15-ms conditioning pulse to +60 mV. The fluorescence signal, but not ionic current during the test pulse has been truncated for purposes of clarity. The dashed lines mark the conditioning pulse instantaneous ion current (in A) or fluorescence amplitude (in B) for comparison. (C) Fractional recovery of the dequenching component of fluorescence amplitude (filled symbols) or the recovery of instantaneous current (open symbols) recorded from three different oocytes during test pulses applied at different intervals following 15-ms conditioning pulses. Data are shown as mean ± SEM. When fitted with a single exponential function, the instantaneous current recovery had a time constant of 10.7 ± 0.8 ms and that of fluorescence was significantly slower 20.7 ± 3.7 ms ($P < 0.05$, $n = 3$).

DISCUSSION

Kv1.5 Fluorescence Recording from A397C

In this description of the first fluorescence reports of the conformational rearrangements associated with gating of a mammalian Kv1 channel, we observed complex fluorescence changes in the report of voltage sensor movements in Kv1.5 channels. Unlike in the *Shaker* channel, the rapid fluorescence quenching associated with activation of the voltage sensors upon depolarization was followed by a rapid dequenching of the fluorescence signal (Fig. 2). Furthermore, this fluorescence

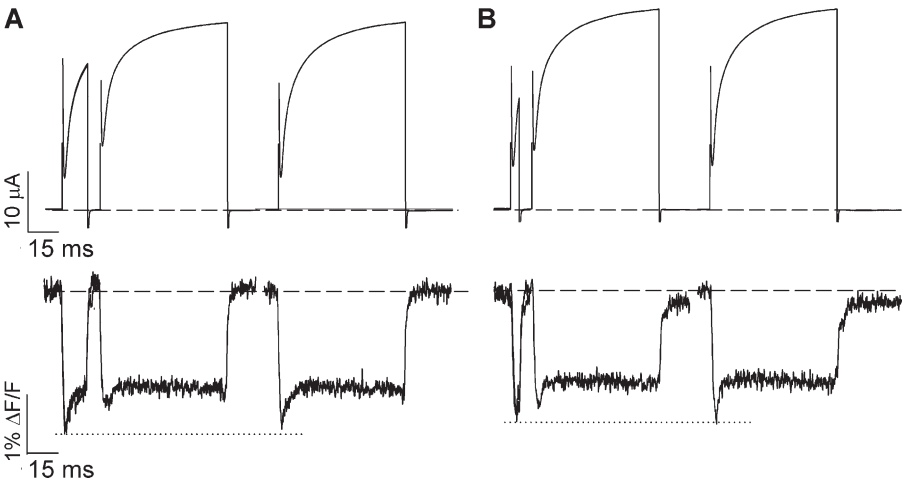

Figure 9. Effect of prepulse duration on the time course of fluorescence recovery. (A and B) Ionic current and fluorescence signals recorded from TMRM-labeled Kv1.5 A397C channels during a 75-ms test pulse to +60 mV applied 7.5 ms and 37.5 ms following a +60-mV conditioning pulse of either 15 ms (A) or 5 ms (B) duration. The dotted line marks the conditioning pulse peak fluorescence amplitude for comparison.

profile was reported by two different fluorophore probes, TMRM and PyMPO (Figs. 2 and 5). This complex report of environmental changes occurring around the fluorophore attached at A397C (and M394C) upon depolarization (Figs. 2–5) suggests unique and complex motions of the voltage sensor domains in Kv1.5 channels that, at face value, are quite different from those reported in *Shaker* channels (Mannuzzu et al., 1996; Cha and Bezanilla, 1997). However, only sites that face the pore domain (A397C and M394C) report the complex changes; many of the sites that do not report the rapid dequenching of fluorescence have F-V relations that are well left shifted from the G-V relations (the $V_{1/2}$ values for the F-V relations of S395C, L396C, and L399C were 64, 12, and 48 mV left shifted from the corresponding $V_{1/2}$ values for the G-V relations) as would be predicted for a faithful report of *Shaker*-like voltage sensor movement (Fig. 3). Furthermore, prevention of the dequenching component of fluorescence from TMRM at A397C (Fig. 7, Fig. 10 D, and Fig. 11 D) unmasks a monophasic *Shaker*-like report of voltage sensor movement. Taken together, these observations suggest that although the fluorescence report from Kv1.5 channels is unique and unusual, voltage sensor movement per se in Kv1.5 channels is not dramatically different from that in the *Shaker* channel.

Clearly however, the data from Fig. 4 demonstrate that the fluorescence signal from TMRM attached to the S3−S4 linker reflects a voltage-dependent channel rearrangement that occurs rapidly at depolarized potentials (τ = 3.4 ms at +60 mV) and is relatively slow to recover (τ = 21 ms; Fig. 8 C). The observation that a

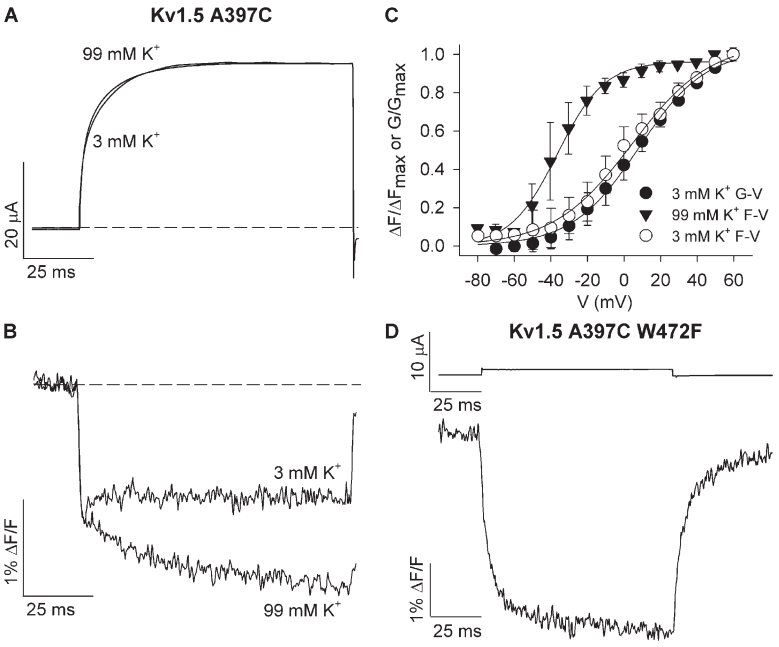

Figure 10. Immobilization of the selectivity filter gate abolishes the fluorescence dequenching. (A and B) Ionic current and fluorescence signals recorded from Kv1.5 A397C channels during 100-ms pulses to +60 mV in the presence of 3 and 99 mM external K^+. (C) Mean F-V relation with 99 mM K^+ plotted alongside the G-V and F-V relations obtained with 3 mM K^+ to demonstrate the voltage dependence of voltage sensor movement when the selectivity filter gate is immobilized by high external K^+. The G-V relation with 99 mM K^+ is not shown because of the large error associated with calculations around the reversal potential (∼0 mV). $V_{1/2}$ and k values for the F-V relation with 99 mM K^+ were −36.4 ± 1.2 and 12.8 ± 1.0 mV, respectively (n = 3). $V_{1/2}$ and k values for the G-V and F-V relations with 3 mM K^+ were 8.1 ± 2.5 and 18.3 ± 1.7 mV (G-V) and 4.3 ± 2.0 and 21.5 ± 1.3 mV (F-V), respectively (n = 3). The F-V relation with high external K^+ was therefore 40 mV left shifted from the G-V relation. (D) Ionic current and fluorescence signals from Kv1.5 A397C W472F mutant channels (W472F is equivalent to the W434F mutation in *Shaker* channels) during a 100-ms voltage clamp pulse from −80 to +60 mV. Note that only small leak currents were observed from oocytes injected with Kv1.5 A397C W472F. Similar recordings were obtained from nine (W472F) other cells.

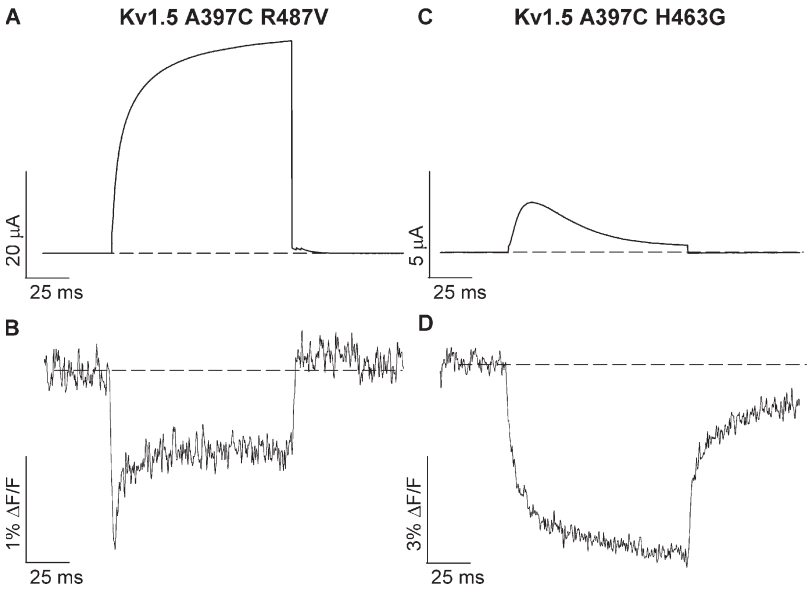

Figure 11. Immobilization of the selectivity filter gate abolishes the fluorescence dequenching. (A and B) Representative fluorescence signals recorded from Kv1.5 A397C R487V mutant channels during a 100-ms voltage clamp pulse from −80 to +60 mV. Similar recordings were obtained from four (R487V) or nine (W472F) other cells. (C and D) Fluorescence signals recorded from Kv1.5 A397C H463G mutant channels during a 100-ms voltage clamp pulse from −80 to +60 mV. Similar recordings were obtained from four (R487V) or five (H463G) other cells.

monoexponential report could be unmasked by manipulation of channel gating processes (Fig. 7, Fig. 10 D, and Fig. 11 D) suggests that the rapid secondary movement occurs to, or close by, the voltage sensor. This dequenches the fluorescence signal, and it occurs in addition to the rapid activation of the voltage sensors upon depolarization that is reported by the initial quenching of the fluorescence signal. In other words, the fluorescence report from Kv1.5 A397C is a composite report of more than one gating event. So what then does the secondary dequenching phase of fluorescence reflect?

The Secondary Dequenching Phase of Fluorescence from Kv1.5 A397C

We presented a series of experiments that strongly suggest that the secondary phase of fluorescence from TMRM-labeled Kv1.5 channels upon depolarization is a report of a gating event that is associated with channel opening (Fig. 2 F and Figs. 4, 6, and 7). By manipulating the holding potential, we demonstrated that labeled channels continued to display a robust secondary dequenching component when activated from preopening potentials (Fig. 6). This suggests that this phase of fluorescence reflects transitions late in the activation pathway that are associated with concerted opening of the channel, or even later events. This is further supported by evidence that binding of 4-AP or introduction of the ILT triple mutations, which both stabilize channels in the activated-not-open state upon depolarization without greatly altering early activation transitions (McCormack et al., 1994; Smith-Maxwell et al., 1998a,b; Armstrong and Loboda, 2001; Loboda and Armstrong, 2001; del Camino et al., 2005), abolished the dequenching of fluorescence (Fig. 7). This conclusion is consistent with electrophysiological and crystallographic data, which demonstrate that each voltage sensor comes into close proximity with the outer pore S5-P linker of its adjacent subunit upon depolarization (Blaustein et al., 2000; Gandhi et al., 2000; Larsson and Elinder, 2000; Li-Smerin et al., 2000; Loots and Isacoff, 2000; Ortega-Saenz et al., 2000; Elinder et al., 2001; Laine et al., 2003; Long et al., 2005b), and is supported by previous observations of structural changes reported by sites within the S3–S4 linker that are associated with opening of the intracellular gate and/or inactivation of the outer pore (Loots and Isacoff, 1998, 2000; Gandhi et al., 2000; Smith and Yellen, 2002; Pathak et al., 2005; Savalli et al., 2006; Claydon et al., 2007a,b).

The W434F mutation in *Shaker* channels (equivalent to W472F in Kv1.5) permanently immobilizes the selectivity filter gate in the P-type inactivated conformation (Perozo et al., 1993; Yang et al., 1997). However, in the absence of K^+, channels are capable of conducting Na^+ (Starkus et al., 1998; Wang and Fedida, 2001). This demonstrates the preservation of intracellular pore gate functionality in W434F/W472F mutant *Shaker* and Kv1.5 channels despite the effects at the selectivity filter gate. Our observation in Fig. 10 D that the W472F mutation abolishes the rapid dequenching component of fluorescence in Kv1.5 channels suggests therefore that the secondary dequenching represents a gating event taking place at the selectivity filter gate rather than the intracellular pore gate, since it is the outer pore gate and not the inner pore gate that is immobilized in this channel. The rapid Kv1.5 fluorescence signal does not reflect channel opening per se, but events at the selectivity filter that occur rapidly upon opening. Because W472F channels are thought to be P-type inactivated at rest (which is why they are nonconducting to K^+), as are the majority of H463G channels (Fig. 11, C and D), these observations raise the possibility that the rapid dequenching event is related to the onset of P-type inactivation in the channels.

An Outer Pore Regulatory Event upon Opening, or More Specifically P-type Inactivation?

Secondary fluorescence deflections associated with rearrangements of the outer pore that occur in addition to activation of the voltage sensors upon depolarization have been previously reported from the equivalent site to A397C (A359C) in *Shaker* channels (Loots and Isacoff, 1998, 2000; Cha and Bezanilla, 1998; Claydon et al., 2007a,b). However, the rapid phase of fluorescence dequenching that we report in the present study from Kv1.5 channels is three orders of magnitude faster than the slow secondary movement associated with P/C-type inactivation reported by the fluorescence signal from *Shaker* A359C, and is only reflected by one side of the S3–S4 linker α-helix, whereas inactivation rearrangements in *Shaker* are sensed by all faces of the S3–S4 linker helix (Figs. 2 and 3) (Loots and Isacoff, 1998, 2000; Claydon et al., 2007b). As well, fluorescence events associated with P/C-type inactivation reported by *Shaker* A359C or Kv1.5 A397C (Claydon et al., 2007b) usually result in a slow phase of fluorescence quenching, as also seen in the present study in Kv1.5 A397C H463G (Fig. 11 D), rather than a rapid phase of fluorescence dequenching. Finally, and importantly, there is no obvious rapid inactivation of ionic current evident in Kv1.5 current traces with the time course of the rapid fluorescence event (e.g., Fig. 2 D). These discrepancies suggest that the rapid dequenching component reported by TMRM and PyMPO attached in Kv1.5 is not simply a report of outer pore movements associated with channel inactivation.

Although we observed that increased K^+ at an outer pore regulatory site, and P-type immobilization of the selectivity filter gate in the mutation W472F, and H463G prevented the fluorescence dequenching (Figs. 10 and 11), the inability of the outer pore mutation R487V (Lopez-Barneo et al., 1993), which inhibits inactivation, to prevent this rapid component of fluorescence (Fig. 11 A) supports the idea that the rapid fluorescence dequenching does not represent the movements associated with P/C-type inactivation in this channel. This last observation must be interpreted with care, as in Kv1.5, the mutation R487V inhibits some events associated with P/C-type inactivation, but not all of them (Fedida et al., 1999; Wang et al., 2000b). Thus, the event may reflect a preinactivation transition that is not prevented by the outer pore mutation R487V.

Alternatively, the observations that raising external K^+ and not the R487V mutation prevented the secondary fluorescence signal (Fig. 10, A–C, and Fig. 11) may also suggest that the rapid dequenching of fluorescence reflects dynamics associated with occupancy of the selectivity filter K^+ modulatory site. It is well known that Kv channel selectivity filter occupancy is modulated by a K^+ binding site within the outer pore (Pardo et al., 1992; Lopez-Barneo et al., 1993; Baukrowitz and Yellen, 1995; Rasmusson et al., 1995; Kiss and Korn, 1998). Our fluorescence data suggest that K^+ exit from its modulatory site within the selectivity filter is associated with local rearrangements that are sensed by the fluorophore attached within the S3–S4 linker region. However, although raised external K^+ caused an appropriate hyperpolarizing shift of the F-V relation (Fig. 10 B), the fluorescence report in raised extracellular K^+ appeared biphasic and was not entirely *Shaker*-like, so it is not entirely clear at this time whether or not K^+ is specifically inhibiting the dequenching event.

This work was supported by grants from the Heart and Stroke Foundation of British Columbia and Yukon and the Canadian Institutes of Health Research to D. Fedida. D. Fedida is supported by a Career Investigator award from the Heart and Stroke Foundation of British Columbia and Yukon. T.W. Claydon was supported by a postdoctoral research fellowship funded by a Focus on Stroke strategic initiative from The Canadian Stroke Network, the Heart and Stroke Foundation, the CIHR Institute of Circulatory and Respiratory Health, and the CIHR/Rx&D Program along with AstraZeneca Canada. M. Vaid was supported by a Michael Smith Foundation for Health Research Studentship. S. Rezazadeh was supported by a Heart and Stroke Foundation of British Columbia and Yukon Studentship and a University of British Columbia Graduate Fellowship.

Olaf S. Andersen served as editor.

Submitted: 30 January 2008
Accepted: 19 June 2008

REFERENCES

Armstrong, C.M., and A. Loboda. 2001. A model for 4-aminopyridine action on K channels: similarities to tetraethylammonium ion action. *Biophys. J.* 81:895–904.

Bannister, J.P., B. Chanda, F. Bezanilla, and D.M. Papazian. 2005. Optical detection of rate-determining ion-modulated conformational changes of the *ether-a-go-go* K^+ channel voltage sensor. *Proc. Natl. Acad. Sci. USA.* 102:18718–18723.

Baukrowitz, T., and G. Yellen. 1995. Modulation of K^+ current by frequency and external $[K^+]$: a tale of two inactivation mechanisms. *Neuron.* 15:951–960.

Blaustein, R.O., P.A. Cole, C. Williams, and C. Miller. 2000. Tethered blockers as molecular "tape measures" for a voltage-gated K^+ channel. *Nat. Struct. Biol.* 7:309–311.

Bruening-Wright, A., F. Elinder, and H.P. Larsson. 2007. Kinetic relationship between the voltage sensor and the activation gate in spHCN channels. *J. Gen. Physiol.* 130:71–81.

Castle, N.A., S.R. Fadous, D.E. Logothetis, and G.K. Wang. 1994. 4-Aminopyridine binding and slow inactivation are mutually exclusive in rat Kv1.1 and *Shaker* potassium channels. *Mol. Pharmacol.* 46:1175–1181.

Cha, A., and F. Bezanilla. 1997. Characterizing voltage-dependent conformational changes in the *Shaker* K^+ channel with fluorescence. *Neuron.* 19:1127–1140.

Cha, A., and F. Bezanilla. 1998. Structural implications of fluorescence quenching in the *Shaker* K^+ channel. *J. Gen. Physiol.* 112: 391–408.

Cha, A., P.C. Ruben, A.L. George Jr., E. Fujimoto, and F. Bezanilla. 1999. Voltage sensors in domains III and IV, but not I and II, are immobilized by Na^+ channel fast inactivation. *Neuron.* 22:73–87.

Chen, F.S., D. Steele, and D. Fedida. 1997. Allosteric effects of permeating cations on gating currents during K^+ channel deactivation. *J. Gen. Physiol.* 110:87–100.

Claydon, T.W., M. Vaid, S. Rezazadeh, S.J. Kehl, and D. Fedida. 2007a. 4-aminopyridine prevents the conformational changes associated with P/C-type inactivation in *Shaker* channels. *J. Pharmacol. Exp. Ther.* 320:162–172.

Claydon, T.W., M. Vaid, S. Rezazadeh, D.C. Kwan, S.J. Kehl, and D. Fedida. 2007b. A direct demonstration of closed-state inactivation of K^+ channels at low pH. *J. Gen. Physiol.* 129:437–455.

Cordero-Morales, J.F., V. Jogini, A. Lewis, V. Vasquez, D.M. Cortes, B. Roux, and E. Perozo. 2007. Molecular driving forces determining potassium channel slow inactivation. *Nat. Struct. Mol. Biol.* 14:1062–1069.

De Biasi, M., H.A. Hartmann, J.A. Drewe, M. Taglialatela, A.M. Brown, and G.E. Kirsch. 1993. Inactivation determined by a single site in K^+ pores. *Pflugers Arch.* 422:354–363.

del Camino, D., M. Kanevsky, and G. Yellen. 2005. Status of the intracellular gate in the activated-not-open state of *Shaker* K^+ channels. *J. Gen. Physiol.* 126:419–428.

Eduljee, C., T.W. Claydon, V. Viswanathan, D. Fedida, and S.J. Kehl. 2007. SCAM analysis reveals a discrete region of the pore turret that modulates slow inactivation in Kv1.5. *Am. J. Physiol. Cell Physiol.* 292:C1041–C1052.

Elinder, F., R. Mannikko, and H.P. Larsson. 2001. S4 charges move close to residues in the pore domain during activation in a K channel. *J. Gen. Physiol.* 118:1–10.

Fedida, D., N.D. Maruoka, and S. Lin. 1999. Modulation of slow inactivation in human cardiac Kv1.5 channels by extra- and intracellular permeant cations. *J. Physiol.* 515:315–329.

Gandhi, C.S., E. Loots, and E.Y. Isacoff. 2000. Reconstructing voltage sensor-pore interaction from a fluorescence scan of a voltage-gated K^+ channel. *Neuron.* 27:585–595.

Gonzalez, C., E. Rosenman, F. Bezanilla, O. Alvarez, and R. Latorre. 2001. Periodic perturbations in *Shaker* K^+ channel gating kinetics by deletions in the S3-S4 linker. *Proc. Natl. Acad. Sci. USA.* 98:9617–9623.

Hoshi, T., W.N. Zagotta, and R.W. Aldrich. 1990. Biophysical and molecular mechanisms of *Shaker* potassium channel inactivation. *Science.* 250:533–538.

Hoshi, T., W.N. Zagotta, and R.W. Aldrich. 1991. Two types of inactivation in *Shaker* K^+ channels: effects of alterations in the carboxy-terminal region. *Neuron.* 7:547–556.

Jäger, H., and S. Grissmer. 2001. Regulation of a mammalian *Shaker*-related potassium channel, hKv1.5, by extracellular potassium and pH. *FEBS Lett.* 488:45–50.

Kehl, S.J., C. Eduljee, D.C. Kwan, S. Zhang, and D. Fedida. 2002. Molecular determinants of the inhibition of human Kv1.5 potassium currents by external protons and Zn^{2+}. *J. Physiol.* 541:9–24.

Kiss, L., and S.J. Korn. 1998. Modulation of C-type inactivation by K^+ at the potassium channel selectivity filter. *Biophys. J.* 74:1840–1849.

Kiss, L., J. LoTurco, and S.J. Korn. 1999. Contribution of the selectivity filter to inactivation in potassium channels. *Biophys. J.* 76:253–263.

Kurata, H.T., and D. Fedida. 2006. A structural interpretation of voltage-gated potassium channel inactivation. *Prog. Biophys. Mol. Biol.* 92:185–208.

Laine, M., M.C. Lin, J.P. Bannister, W.R. Silverman, A.F. Mock, B. Roux, and D.M. Papazian. 2003. Atomic proximity between S4 segment and pore domain in *Shaker* potassium channels. *Neuron.* 39:467–481.

Larsson, H.P., and F. Elinder. 2000. A conserved glutamate is important for slow inactivation in K^+ channels. *Neuron.* 27:573–583.

Li-Smerin, Y., and K.J. Swartz. 2001. Helical structure of the COOH terminus of S3 and its contribution to the gating modifier toxin receptor in voltage-gated ion channels. *J. Gen. Physiol.* 117:205–218.

Li-Smerin, Y., D.H. Hackos, and K.J. Swartz. 2000. α-Helical structural elements within the voltage-sensing domains of a K^+ channel. *J. Gen. Physiol.* 115:33–50.

Loboda, A., and C.M. Armstrong. 2001. Resolving the gating charge movement associated with late transitions in K channel activation. *Biophys. J.* 81:905–916.

Long, S.B., E.B. Campbell, and R. MacKinnon. 2005a. Crystal structure of a mammalian voltage-dependent *Shaker* family K^+ channel. *Science.* 309:897–903.

Long, S.B., E.B. Campbell, and R. MacKinnon. 2005b. Voltage sensor of Kv1.2: structural basis of electromechanical coupling. *Science.* 309:903–908.

Long, S.B., X. Tao, E.B. Campbell, and R. MacKinnon. 2007. Atomic structure of a voltage-dependent K^+ channel in a lipid membrane-like environment. *Nature.* 450:376–382.

Loots, E., and E.Y. Isacoff. 1998. Protein rearrangements underlying slow inactivation of the *Shaker* K^+ channel. *J. Gen. Physiol.* 112:377–389.

Loots, E., and E.Y. Isacoff. 2000. Molecular coupling of S4 to a K^+ channel's slow inactivation gate. *J. Gen. Physiol.* 116:623–636.

Lopez-Barneo, J., T. Hoshi, S.H. Heinemann, and R.W. Aldrich. 1993. Effects of external cations and mutations in the pore region on C-type inactivation of *Shaker* potassium channels. *Receptors Channels.* 1:61–71.

Mannuzzu, L.M., M.M. Moronne, and E.Y. Isacoff. 1996. Direct physical measure of conformational rearrangement underlying potassium channel gating. *Science.* 271:213–216.

McCormack, K., W.J. Joiner, and S.H. Heinemann. 1994. A characterization of the activating structural rearrangements in voltage-dependent *Shaker* K^+ channels. *Neuron.* 12:301–315.

Ortega-Saenz, P., R. Pardal, A. Castellano, and J. Lopez-Barneo. 2000. Collapse of conductance is prevented by a glutamate residue conserved in voltage-dependent K^+ channels. *J. Gen. Physiol.* 116:181–190.

Pardo, L.A., S.H. Heinemann, H. Terlau, U. Ludewig, C. Lorra, O. Pongs, and W. Sthmer. 1992. Extracellular K^+ specifically modulates a rat brain K^+ channel. *Proc. Natl. Acad. Sci. USA.* 89:2466–2470.

Pathak, M., L. Kurtz, F. Tombola, and E. Isacoff. 2005. The cooperative voltage sensor motion that gates a potassium channel. *J. Gen. Physiol.* 125:57–69.

Pathak, M.M., V. Yarov-Yarovoy, G. Agarwal, B. Roux, P. Barth, S. Kohout, F. Tombola, and E.Y. Isacoff. 2007. Closing in on the resting state of the *Shaker* K^+ channel. *Neuron.* 56:124–140.

Perozo, E., R. MacKinnon, F. Bezanilla, and E. Stefani. 1993. Gating currents from a nonconducting mutant reveal open-closed conformations in *Shaker* K^+ channels. *Neuron.* 11:353–358.

Piper, D.R., A. Varghese, M.C. Sanguinetti, and M. Tristani-Firouzi. 2003. Gating currents associated with intramembrane charge displacement in hERG potassium channels. *Proc. Natl. Acad. Sci. USA.* 100:10534–10539.

Rasmusson, R.L., M.J. Morales, R.C. Castellino, Y. Zhang, D.L. Campbell, and H.C. Strauss. 1995. C-type inactivation controls recovery in a fast inactivating cardiac K^+ channel (Kv1.4) expressed in *Xenopus* oocytes. *J. Physiol.* 489:709–721.

Savalli, N., A. Kondratiev, L. Toro, and R. Olcese. 2006. Voltage-dependent conformational changes in human Ca^{2+}- and voltage-activated K^+ channel, revealed by voltage-clamp fluorometry. *Proc. Natl. Acad. Sci. USA.* 103:12619–12624.

Smith, P.L., and G. Yellen. 2002. Fast and slow voltage sensor movements in hERG potassium channels. *J. Gen. Physiol.* 119:275–293.

Smith-Maxwell, C.J., J.L. Ledwell, and R.W. Aldrich. 1998a. Role of the S4 in cooperativity of voltage-dependent potassium channel activation. *J. Gen. Physiol.* 111:399–420.

Smith-Maxwell, C.J., J.L. Ledwell, and R.W. Aldrich. 1998b. Uncharged S4 residues and cooperativity in voltage-dependent potassium channel activation. *J. Gen. Physiol.* 111:421–439.

Starkus, J.G., L. Kuschel, M.D. Rayner, and S.H. Heinemann. 1998. Macroscopic Na^+ currents in the "non-conducting" *Shaker* potassium channel mutant W434F. *J. Gen. Physiol.* 112:85–93.

Wang, Z., and D. Fedida. 2001. Gating charge immobilization caused by the transition between inactivated states in the Kv1.5 channel. *Biophys. J.* 81:2614–2627.

Wang, Z., X. Zhang, and D. Fedida. 1999. Gating current studies reveal both intra- and extracellular cation modulation of K^+ channel deactivation. *J. Physiol.* 515:331–339.

Wang, Z., J.C. Hesketh, and D. Fedida. 2000a. A high-Na^+ conduction state during recovery from inactivation in the K^+ channel Kv1.5. *Biophys. J.* 79:2416–2433.

Wang, Z., X. Zhang, and D. Fedida. 2000b. Regulation of transient Na^+ conductance by intra- and extracellular K^+ in the human delayed rectifier K^+ channel Kv1.5. *J. Physiol.* 523:575–591.

Yang, Y., Y. Yan, and F.J. Sigworth. 1997. How does the W434F mutation block current in *Shaker* potassium channels? *J. Gen. Physiol.* 109:779–789.

Yellen, G. 1998. The moving parts of voltage-gated ion channels. *Q. Rev. Biophys.* 31:239–295.

Zhang, S., C. Eduljee, D.C. Kwan, S.J. Kehl, and D. Fedida. 2005. Constitutive inactivation of the hKv1.5 mutant channel, H463G, in K^+-free solutions at physiological pH. *Cell Biochem. Biophys.* 43:221–230.